

Cite this: DOI: 10.1039/xxxxxxxxxx

Supporting Information Structural changes in equimolar ceria-hafnia materials under solar thermochemical looping conditions: cation ordering, formation and stability of the pyrochlore structure[†]

Matthäus Rothensteiner,^{a,b} Alexander Bonk,^{c,d} Ulrich F. Vogt,^{c,d} Hermann Emerich^e, and Jeroen A. van Bokhoven^{*a,b}

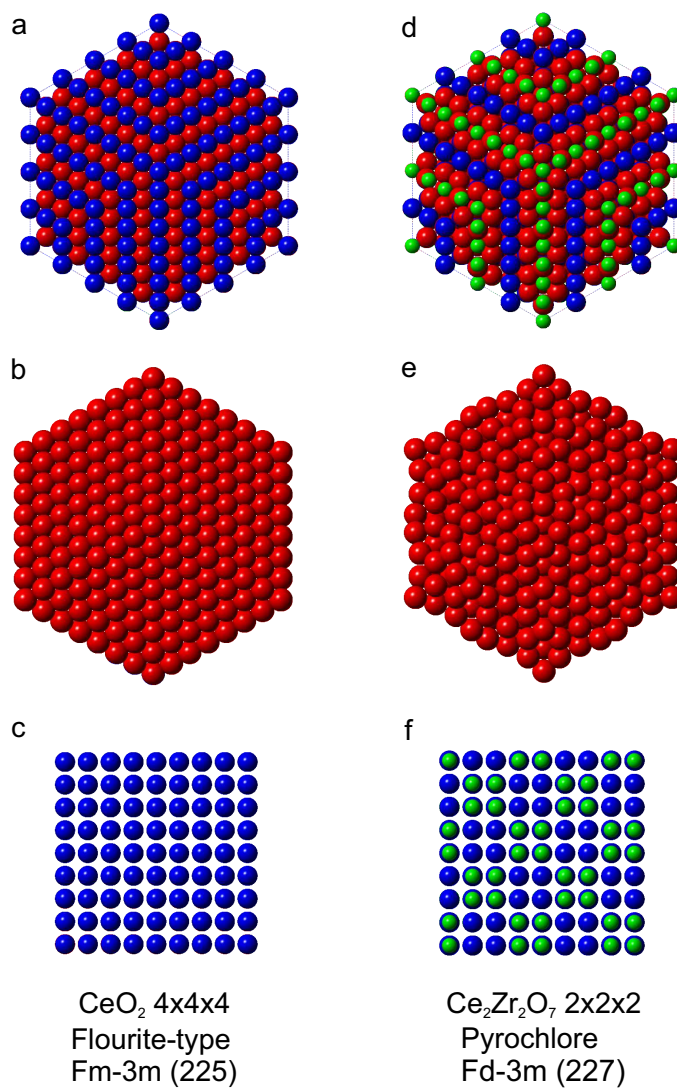


Fig. S1 1 Arrangement of cerium (blue), oxygen (red), and zirconium (green) ions in the cubic fluorite-type (a-c) and the pyrochlore (d-f) structures. Views of supercells in direction of the diagonal [111] direction in a,b,d and e) and the x axis N(100) in c) and f), illustrating the ordered arrangement of cations in the pyrochlore-type structure.

| Ce ₂ Zr ₂ O ₇ Sasaki et al ¹ | | | auto-reduced Hf50 (TGA) | | | | | |
|--|---|---|-------------------------|-----------|-------|-----------|-----------------|--|
| h | k | l | 2θ | Intensity | 2θ | Intensity | Intensity ratio | |
| 1 | 1 | 1 | 14.26 | 2.58 | 14.30 | 1.94 | 0.75 | |
| 2 | 2 | 0 | 23.39 | 0.08 | a | a | | |
| 3 | 1 | 1 | 27.51 | 1.20 | 27.60 | 2.27 | 1.89 | |
| 2 | 2 | 2 | 28.76 | 100.00 | 28.85 | 100.00 | 1.00 | |
| 4 | 0 | 0 | 33.32 | 31.45 | 33.44 | 32.90 | 1.05 | |
| 3 | 3 | 1 | 36.42 | 4.89 | 36.53 | 0.11 | 0.02 | |
| 4 | 2 | 2 | 41.10 | 0.29 | 41.30 | 0.21 | 0.72 | |
| 5 | 1 | 1 | 43.73 | 2.05 | 43.91 | 0.78 | 0.38 | |
| 3 | 3 | 3 | 43.73 | * | * | * | * | |
| 4 | 4 | 0 | 47.83 | 51.99 | 48.02 | 33.73 | 0.65 | |
| 5 | 3 | 1 | 50.16 | 1.04 | 50.37 | 0.45 | 0.43 | |
| 4 | 4 | 2 | 50.94 | 0.00 | a | a | | |
| 6 | 2 | 0 | 53.91 | 0.08 | a | a | | |
| 5 | 3 | 3 | 56.07 | 0.15 | 56.29 | 0.32 | 2.13 | |
| 6 | 2 | 2 | 56.78 | 47.16 | 57.00 | 25.22 | 0.53 | |
| 4 | 4 | 4 | 59.53 | 10.76 | 59.79 | 6.06 | 0.56 | |
| 5 | 5 | 1 | 61.57 | 0.60 | 61.81 | 0.28 | 0.46 | |
| 7 | 1 | 1 | 61.57 | * | * | * | * | |
| 6 | 4 | 2 | 64.86 | 0.00 | a | a | | |
| 5 | 5 | 3 | 66.82 | 0.45 | 67.08 | 0.32 | 0.70 | |
| 7 | 3 | 1 | 66.82 | * | * | * | * | |
| 8 | 0 | 0 | 69.97 | 7.64 | 70.25 | 2.70 | 0.35 | |
| 7 | 3 | 3 | 71.85 | 0.84 | a | a | | |
| 6 | 4 | 4 | 72.45 | 0.00 | a | a | | |
| 6 | 6 | 0 | 74.90 | 0.21 | a | a | | |
| 8 | 2 | 2 | 74.90 | * | * | * | * | |
| 7 | 5 | 1 | 76.73 | 0.27 | a | a | | |
| 5 | 5 | 5 | 76.73 | 0.19 | a | a | | |
| 6 | 6 | 2 | 77.34 | 18.51 | 77.66 | 5.99 | 0.32 | |
| 8 | 4 | 0 | 79.73 | 14.57 | 80.09 | 4.70 | 0.32 | |

Table S1 Numerical details of XRD of Hf50 after auto-reduction in the TGA experiment compared to literature data¹ of ceria-zirconia pyrochlore. Asterisks (*) indicate that intensities of reflections at identical Bragg angles were added up. (a) indicates reflections that were not observed in the pattern of auto-reduced Hf50.

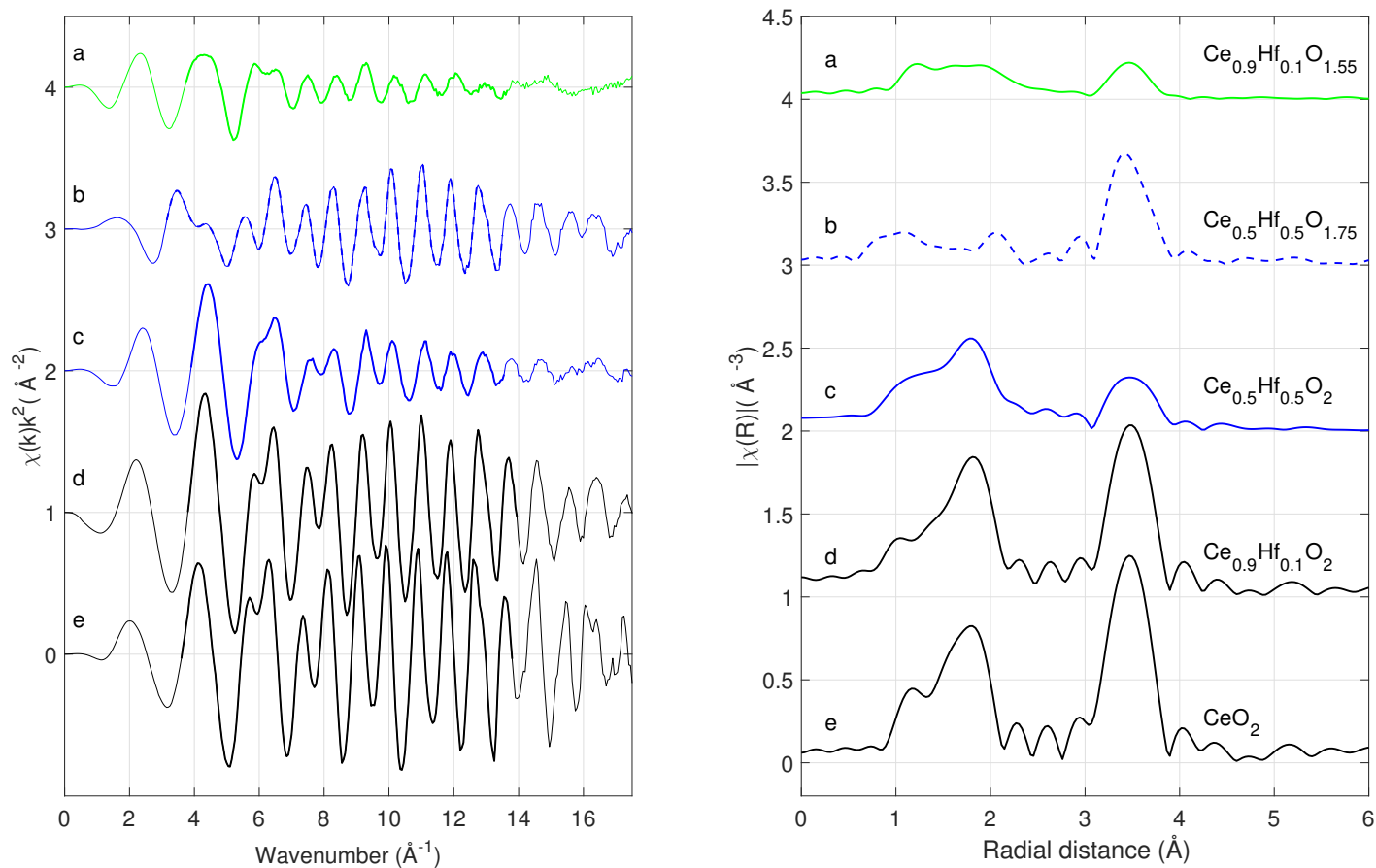


Fig. SI 2 Ce K edge EXAFS signals recorded at room temperature before and after auto-reduction and relevant reference spectra. Bold lines indicate the k -range used in the Fourier transform. Comparison to spectra recorded in earlier experiments². EXAFS analysis is hampered by an intense and broad glitch at $k = 9.3 \text{ \AA}^{-1}$ that corrupted the signal.

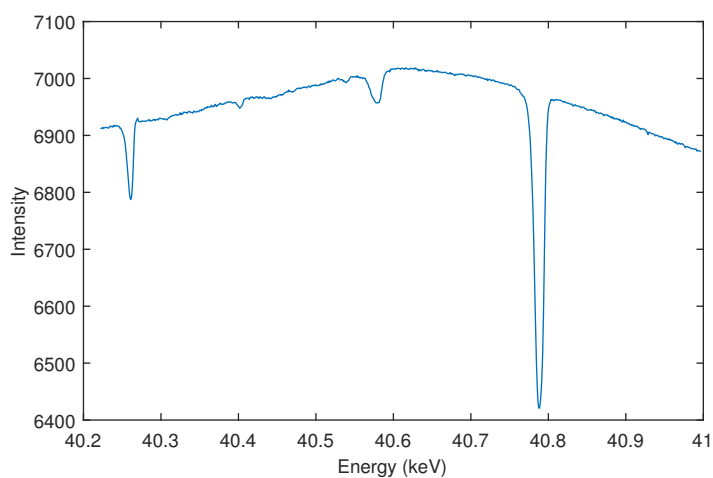


Fig. SI 3 EXAFS fitting of Ce K edge data collected at room temperature was complicated by a very strong and broad glitch that severely corrupted the signal. The incident intensity I_0 as a function of the photon energy containing three strong glitches at 40.260, 40.578 and 40.787 keV. The glitch at 40.787 keV had a FWHM of 12 eV. In addition, thermal treatment often affects the quality of the pellets which is detrimental to the quality of the XAS signal. Thus, despite very good signal/noise ratios up to very high wave-numbers, reliable results from Ce K edge EXAFS were not accessible.

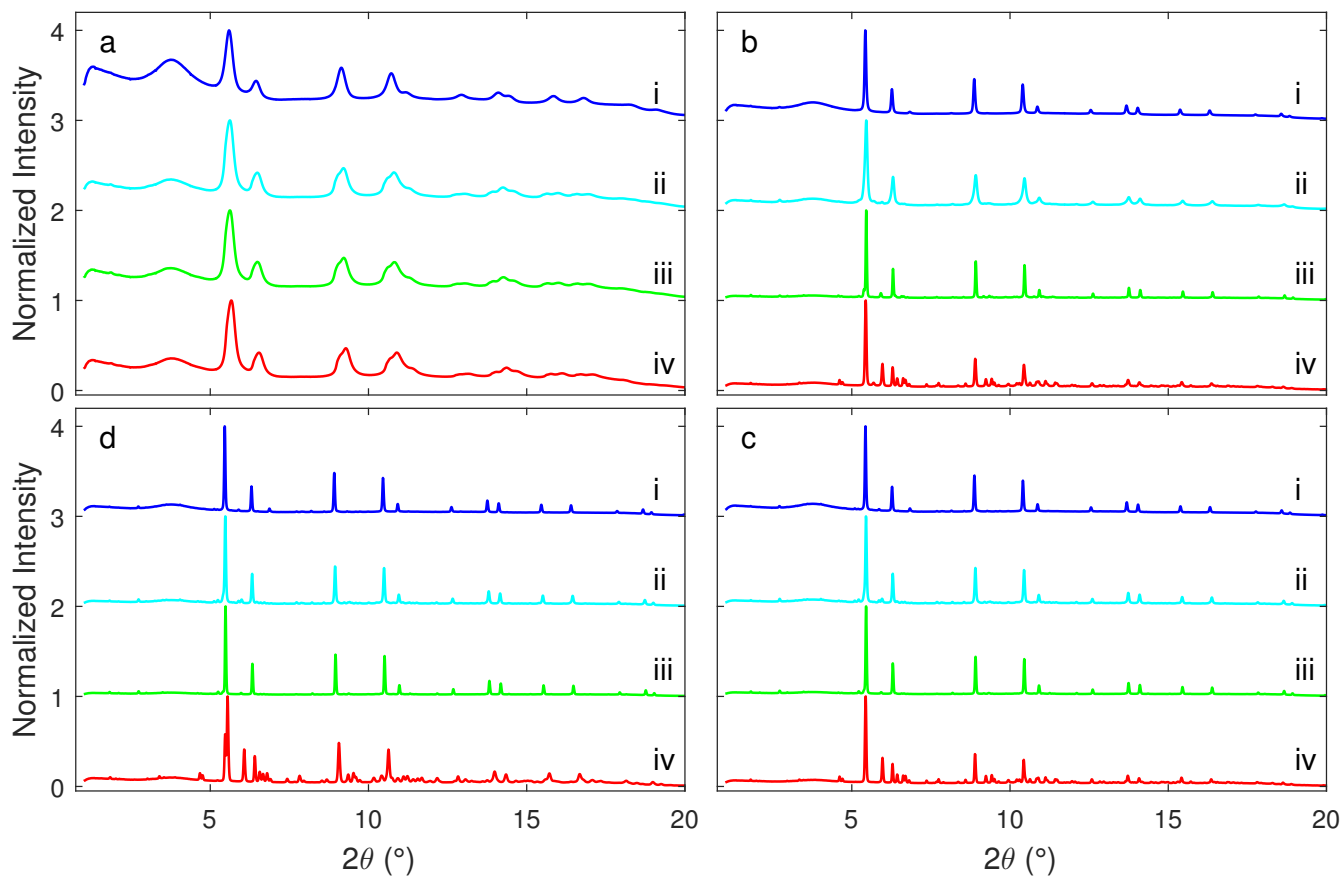


Fig. S1 4 Normalized XRD patterns recorded with a focused beam before, during and after high temperature treatment of i) Zr50C in a flow of hydrogen/helium, ii) Hf50C in a flow of hydrogen/helium iii) Hf50C in a flow of argon and iv) Hf50C in air; a) at room temperature before heating b) at the end of the heating ramp, c) after 30 minutes at the maximum temperature (1623 ± 50 K in hydrogen/helium and 1823 ± 50 K in argon and air) before cooling and d) after the thermal treatment at room temperature.

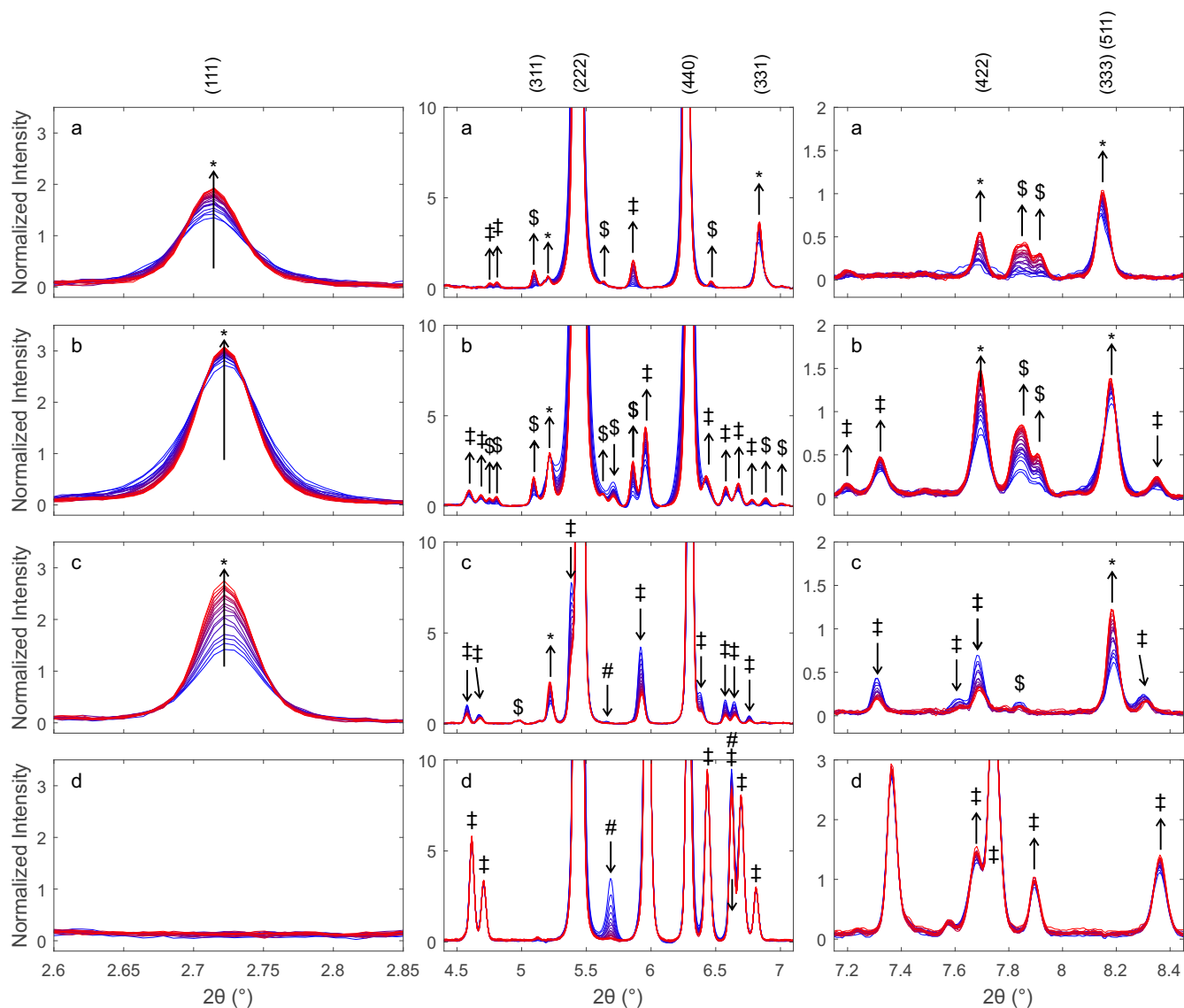


Fig. SI 5 Details of normalized XRD patterns highlighting reflections of the pyrochlore structure. Patterns were recorded during 30 min at constant temperature after heating a) Zr50C in hydrogen/helium, b) Hf50C in hydrogen/helium, c) Hf50C in argon and d) Hf50C in air at 50 K/min (see Figure ??). In hydrogen/helium the maximum temperature was 1623 ± 50 K and it was 1823 ± 50 K in argon and air. Blue indicates the first and red the last diffraction pattern. The background was subtracted prior to normalization. Arrows indicate changes in the intensities of reflections assigned to the pyrochlore phase.

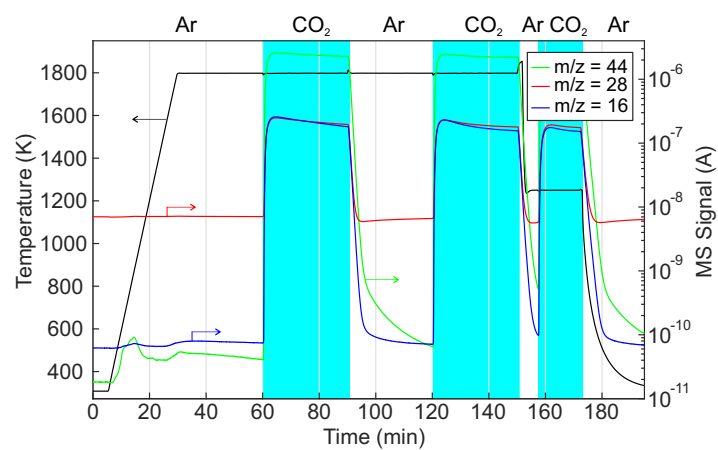


Fig. SI 6 Temperature profile and MS signals in the isothermal carbon dioxide splitting experiment for in situ XRD. Hf50C, auto-reduced thermally in a flow of argon and subsequently decorated with platinum, was exposed to isothermal carbon dioxide splitting conditions at 1800 ± 50 K. The gas flow rates were 200 mL/min argon and 100 ml/min carbon dioxide.

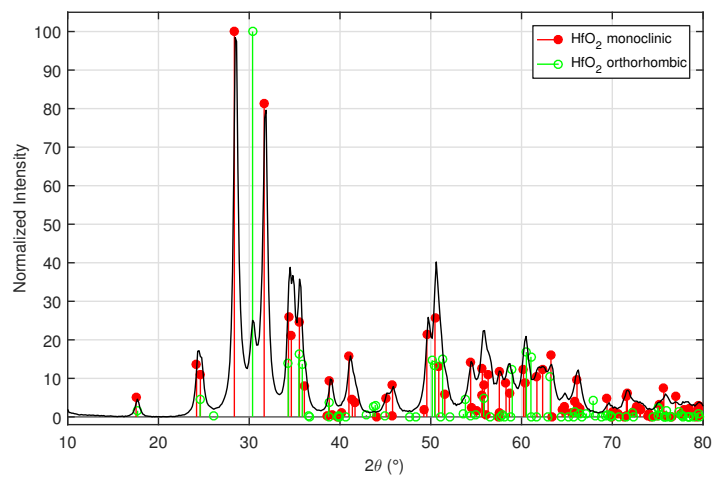


Fig. SI 7 Powder XRD pattern of the HfO₂ reference (Alfa Aesar, 99.95%) and X-ray diffraction literature data of monoclinic (ICSD # 60902) and orthorhombic (ICSD # 71354) hafnia.

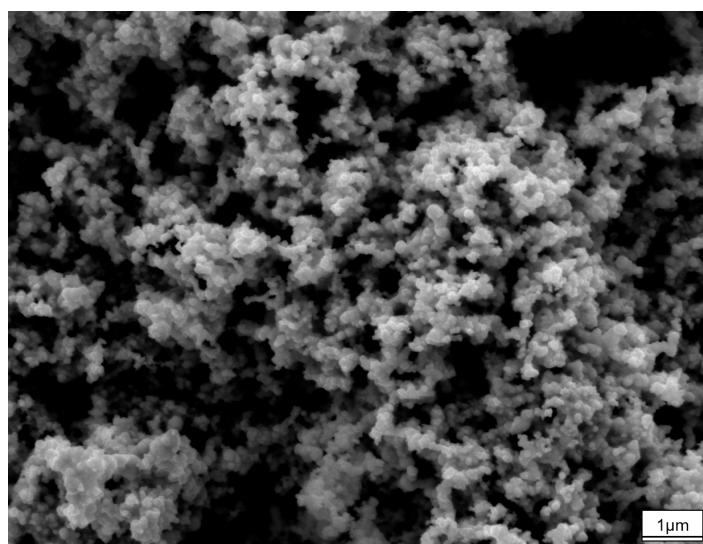


Fig. SI 8 SEM image of HfO₂ reference (Alfa Aesar, 99.95%) recorded at a magnification of 20k and 10 kV.

References

- 1 T. Sasaki, Y. Ukyo, K. Kuroda, S. Arai, S. Muto and H. Saka, *Journal of the Ceramic Society of Japan*, 2004, **112**, 440–444.
- 2 M. Rothensteiner, S. Sala, A. Bonk, U. Vogt, H. Emerich and J. A. van Bokhoven, *Phys. Chem. Chem. Phys.*, 2015, **17**, 26988–26996.